Numerical study of microwave discharge ion thruster µ10

IEPC-2019-218

Yusuke Yamashita[1] and Yoshitaka Tani[2]
The University of Tokyo, Tokyo, 113-8656, Japan

Ryudo Tsukizaki[3], Koda Daiki[4], Kazutaka Nishiyama[5] Hitoshi Kuninaka[6]

Japan Aerospace Exploration Agency, 3-1-1, Kanagawa 252-5210, Japan

We report the performance limitation of the microwave discharge ion thruster µ10. In the thruster, the thrust is limited to the propellant flow rate and the thrust decreases drastically if the propellant flow rate increases. To reveal the mechanism, we investigated plasma properties qualitatively using full-PIC simulation. The simulation results indicate that the plasma is generated where electrons are confined and heated by ECR, and we call the region 'active' region in this paper. Then, in previous study, the neutral density is important for the performance limitation. Hence, we roughly evaluated the neutral density distribution with ion acceleration by using DSMC, ion loss current by electrostatic probe measurement, the experimental ion beam current, and distribution of ionization by full-PIC simulation. The result shows that the neutral density increases except for 'active' region, which indicates that the assumption of ionization distribution is violated if the propellant flow rate increases. If the plasma generated except for active region, the excitation loss and wall loss become large due to low electron temperature and no magnetic confinement, which is thought to be the mechanism of the performance limitation. To confirm the hypothesis, we measured the ion current density distribution before and after the performance limitation. From the measurement, the assumption that plasma is generated mainly active region is violated after the performance limitation. In addition, to investigate the relationship between the volume of 'active' region and the performance limitation, we experimented three kinds of the thruster. As a result, the maximum ion beam current corresponds to the volume of 'active' region. Hence, the volume of 'active' region is one of the most important design parameters to improve the performance limitation.

Nomenclature

$\boldsymbol{B_s}$	=	static magnetic field by permanent magnet
$\boldsymbol{E_m}$	=	electric field of microwaves
$\boldsymbol{E_s}$	=	electrostatic field
I_b	=	ion beam current
I_p	=	ion production current
I_w	=	ion wall loss current
m	=	mass
n_n	=	neutral density
t	=	time

[1]Graduate student, Department of Aeronautics and Astronautics, yamashita@ep.isas.jax.jp.
[2]Graduate student, Department of Aeronautics and Astronautics, tani@ep.isas.jaxa.jp
[3]Assistant professor, Department of Aeronautics and Astronautics, ryudo@ep.isas.jaxa.jp
[4]Project Researcher, Institute of Space and Astronautical Science, koda@ep.isas.jaxa.jp
[5]Associate Professor, Institute of Space and Astronautical Science, nishiyama@ep.isas.jaxa.jp
[6] Professor, Institute of Space and Astronautical Science, kuninaka@ep.isas.jaxa.jp

v	=	velocity
x	=	position
α	=	coefficient of absorbed power
ω_m	=	microwaves frequency
ϕ	=	electrostatic potential
η_u	=	propellant utilization efficiency
η_{ex}	=	ion extracted efficiency

I. Introduction

Microwave discharge ion thruster μ10 has been developed by Japan Aerospace Exploration Agency (JAXA). The thruster was mounted on Hayabusa, and Hayabusa2[1)].

In addition, the thruster will be mounted on mounted on spacecraft "Hayabusa" and "Hayabusa 2" and has an operation record of over 40,000 hours[2)]. Then, it is planned to be used for Phaethon flyby mission satellite DESTINY+ or the solar powered sail satellite OKEANOS [3),] Therefore, we improve the thruster performance. However, the thrust is limited to the propellant rate, and the thrust decreases drastically if the propellant flow rate increases. In this paper, we performed full-PIC simulation and DSMC simulation, and electrostatic probe measurement to reveal the performance limitation. Firstly, the distribution of ionization rate is qualitatively evaluated by full-PIC simulation. Then, the distribution of neutral density is evaluated by DSMC and ion loss measurement using electrostatic probe. Based on the results, we suggest the hypothesis of the performance limitation. Then, to confirm the hypothesis, we measured the ion current density distribution before and after the performance limitation, and experimented by three kinds of thruster.

II. Qualitative investigation by full-PIC

A. Numerical model

Motion of charged particles is described as follows,

$$m\frac{d\boldsymbol{v}}{dt} = q\left(\alpha \boldsymbol{E_{m,0}} \sin \omega_m t + \boldsymbol{E_s} + \boldsymbol{v} \times \boldsymbol{B}\right) \tag{1}$$

$$\frac{d\boldsymbol{x}}{dt} = \boldsymbol{v} \tag{2}$$

In case of ions, $\boldsymbol{E_{m,0}}$ is neglected because ion plasma frequency is very larger than that of microwaves. Then, eq. (1) is solved by Boris method[6)], and eq. (2) is solved by leap flog method. The time step of the electrons Δt_e is 5.95×10^{-12}s. and the time step of the ions Δt_i is 2.38×10^{-10}s to save the simulation time.

Then, to solve the electrostatic field, the following Poisson equation is solved.

$$\left(\frac{\partial^2}{\partial r^2} + \frac{1}{r}\frac{\partial}{\partial r} + \frac{\partial^2}{\partial z^2}\right)\phi = -\frac{\rho_i - \rho_e}{\epsilon_0} \tag{3}$$

$$\boldsymbol{E_s} = -\nabla\phi \tag{4}$$

In this case, the position of charged particles in the azimuthal direction is neglected to save simulation time. From reference 7, 1 cm class microwave ion thruster has time oscillation of electrostatic field in azimuthal direction. Hence, we evaluate only the time averaged value. Eq. (3) is solved by Successive Over-Relaxation (SOR) method[8)].

Collision between neutral particles and electrons is solved by Monte Carlo Collision (MCC). The collision between neutral particles and electrons is considered, and the collision between ions and neutral particles are neglected. In addition, we consider three collisions, ionization, excitation, and elastic collision. In order to save simulation time, Null collision method is applied to the collision [9)]. In this simulation, neutral density is assumed to be $n_n = 10^{19}\mathrm{m}^{-3}$ with temperature of 300 K, and uniform in simulation area.

The velocity after collision is simulated based on the energy and momentum conservation. Time step of collision Δt_c is 2.38×10^{-10}s. Finally, to analyze the electromagnetic field of microwaves, we use Finite Difference Time Domain (FDTD) method. In this study, the change of phase by plasma current is neglected. Then, to adjust the intensity of microwaves, coefficient α is adjusted to meet the absorbed power which is the time change of the energy of plasma and the input power[10)]. In this simulation, absorbed power is set 12 W. These simulations are continued until the plasma density and electron temperature is steady state.

B. Distribution of ionization rate

The simulation results indicate that the number density of plasma is order of $10^{17}\ m^{-3}$ in the confined region. On the other hand, the number density of plasma is order of $10^{16}\ m^{-3}$ in other regions. In addition, the electron temperature is 15 eV in the confinement region, and about 1-5 eV in other regions. These structures are confirmed by Langmuir probe measurement[11]. The ionization rate is shown Fig.1. The figure indicates that the ionization rate is highest near the ECR layer. The causes are thought to be that electrons are heated and strongly confined in this region. Hence, the ionization is mainly occurred in the confined region. In this paper, we call the region where electrons are confined and heated by ECR 'active' region like Fig.2. Detailed results are shown in reference 12.

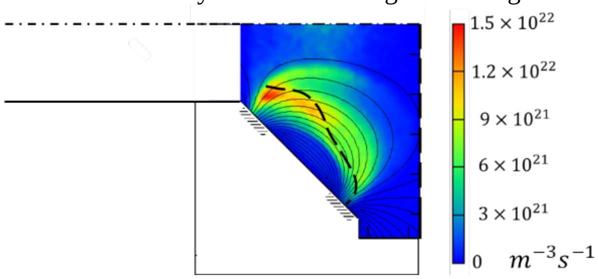

Figure.1 Distribution of time-averaged ionization rate

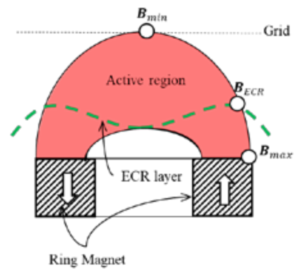

Figure.2 'Active' region

III.Quantitative evaluation of neutral density by DSMC, electrostatic probe, ion beam current

A. Numerical model

To evaluate the distribution of neutral density, we use both the simulation and experimental data of electric static probe. The simulation model is shown in Fig.3. Continuity equation of ions and neutral atoms can be expressed as follows.

$$\dot{m}_{out} = \dot{m}_{in} - I_b \tag{5}$$

$$\dot{m}_{out} = \dot{m}_{in} + \frac{(1-\eta_{ex})}{\eta_{ex}} I_b - \frac{1}{\eta_{ex}} I_b \tag{6}$$

$$\dot{m}_{out} = \dot{m}_{in} + I_w - I_p \tag{7}$$

Here, I_w is ion wall loss current, and I_p is ionization rate. Hence, to get the neutral density distribution with ion acceleration, ion wall loss current distribution, and the ionization rate is needed. In the experiment, the ion beam current can be measured. In addition, ion wall current distribution I_w and extracted efficiency η_{ex} are measured by electrostatic probes[13]. By using the experimental data, the ion wall current distribution and amount of ionization rate can be evaluated. However, the position of ionization can't be determined. In this study, the distribution of ionization is assumed to be only 'active' region. The assumption is validated by full-PIC simulation. The simulation flow is shown in Fig.3.

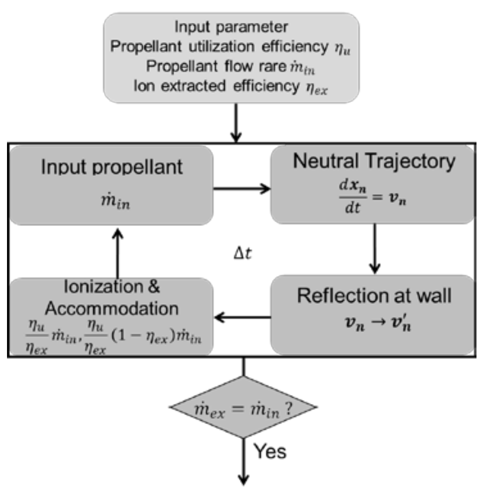

Figure 3. Simulation flow of neutral particles flow with ion acceleration.

B. Distribution of neutral density in Hayabusa and Hayabusa2 operation

In this simulation, we performed Hayabusa and Hayabusa2 operation. In Hayabusa mode, the location of propellant is only waveguide. Then, maximum propellant flow rate is 2.3 sccm, propellant utilization efficiency is 0.8, and extracted efficiency is 0.4. On the other hand, in Hayabusa2 mode, the location of propellant is almost discharge chamber. Then, maximum propellant flow rate is 3.0 sccm, propellant utilization efficiency is 0.8, and extracted efficiency is 0.36. The ion wall current is quoted from electrostatic probe measurement[13)]. The distribution of the neutral density is shown in Fig. 4. Even if maximum propellant flow rate is different between Hayabusa and Hayabusa2 mode, the maximum neutral density is almost 6.0×10^{18} m^{-3}. Then, the distribution is significantly different from without plasma. In µ10 ion thruster, propellant utilization efficiency is 0.8, and the effect of ionization is very large. Therefore, we need to consider the effect of neutral density distribution with ionization to simulate the ion acceleration mode.

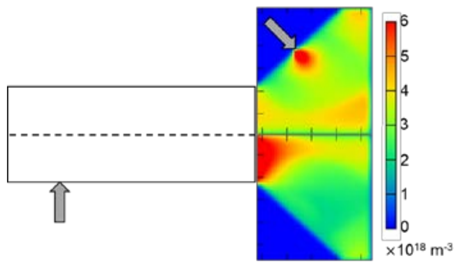

Figure 4. Neutral density distribution with ion acceleration. Above: Hayabusa2, bottom: Hayabusa. The ion wall loss current and operation data are quoted from reference 13.

IV.Confirmation of the performance limitation by measuring the ion current density

A. Hypothesis of the performance limitation

The ion production current which is volume integration of ionization rate can be written $<\sigma v>_{ioni}\, n_n n_e V$. Here, $<\sigma v>_{ioni}$ is reaction rate of the ionization, and V is volume. Based on the result of the neutral density distribution (Fig.4), the neutral density except for 'active' region increases corresponding to propellant flow rate. Hence, the assumption that ionization is mainly occurred in 'active' region is violated if the propellant flow rate increases. Then, if plasma is generated except for 'active' region, the excitation loss and wall loss becomes large due to low electron temperature and no magnetic condiment, which is thought to be mechanism of the performance limitation.

B. Measurement procedure

To confirm the hypothesis, we measured ion current density distribution before and after the performance limitation. The ion current density distribution roughly shows where the plasma is generated. The measurement system is shown in Fig.5. To reflect the electrons from the chamber, the probe is biased -30 V. Then, the probe swipes in the radial direction.

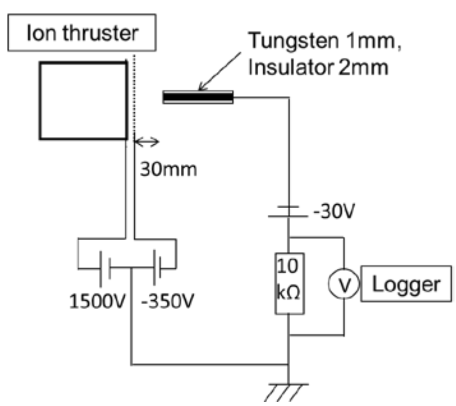

Figure 5. Measurement system of ion current density distribution

C. Ion current density distribution before and after the performance limitation

The ion current density distribution is shown in Fig. 6. Left figure shows the ion current density distribution before the performance limitation, and right figure shows the results after the performance limitation. 'Active' region is 30~50 mm. Hence, left figure shows the ion current density is high in 'active' region, which shows that the plasma is mainly generated in 'active' region. However, the right figure shows the ion current density doesn't high, which shows that the plasma isn't manly generated in 'active' region. Based on two results, it is confirmed that the hypothesis is valid.

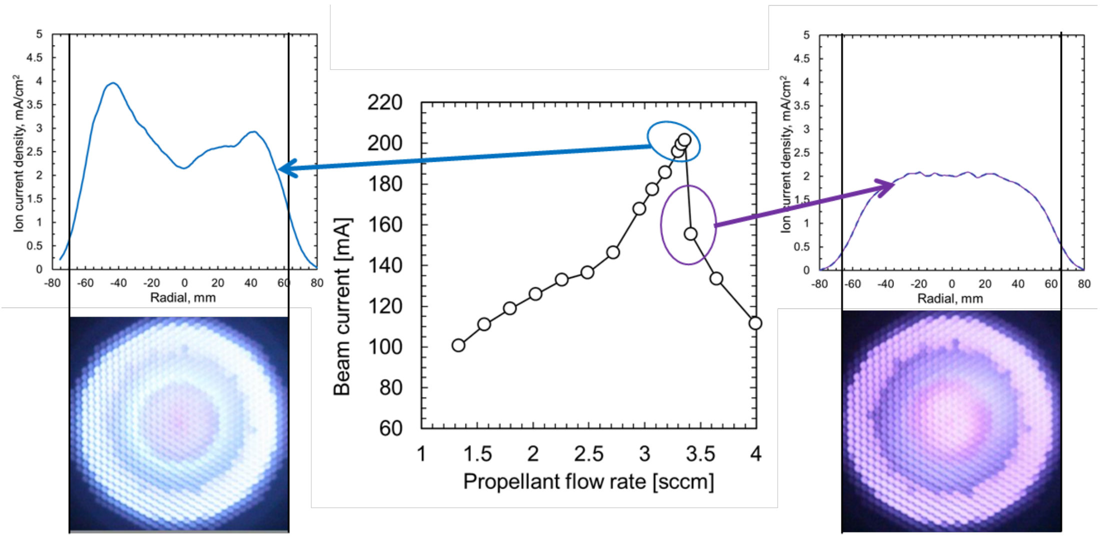

Figure 6. Ion current density distribution before and after the performance limitation. left: before, right: after.

V. Suggestion of key parameter

A. Key parameter

We suggest the key parameter based on above hypothesis. From the hypothesis, ion production current in 'active' region increases, while the current except for 'active' region decreases. The ion production current can be written $<\sigma v>_{ioni} n_n n_e V$, $<\sigma v>_{ioni}$ depends on electron temperature. However, it is difficult to determine the plasma parameter such as electron temperature and density in advance. Hence, we suggest the key parameter volume. If volume of active region increases and that of non-active region decreases, the performance limitation can be improved.

B. Experimental procedure

To confirm the suggestion, we experiment three kinds of thrusters. The geometry is shown in Fig.7. Type A shows that both two magnets are in 45-degree direction, and same as Hayabusa series. Type B shows that upstream magnet is in 45-degree direction, while downstream magnet is in axial direction. Type C shows that both two magnets are in axial direction.

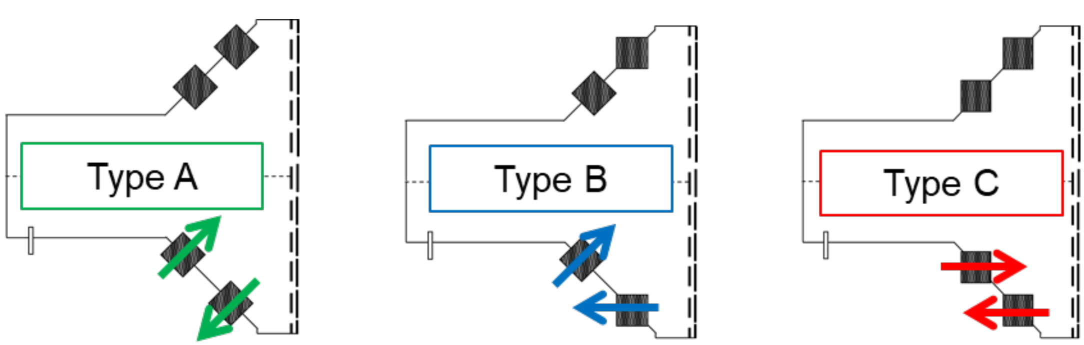

Figure 7. Geometry of three kinds of thruster.

C. Relationship between ion beam current and volume of active region

Three kinds of ion beam current are shown in Fig.8 (a). The results indicate that the maximum ion beam current is B>C>A. While, Fig, 8(b) shows that normalized volume of active region. To normalize the volume, volume of the discharge chamber is used, which is almost same among three thrusters. Then, $H_{discharge}$ is the height of the discharge chamber. '0' mm indicates that the height is same as Hayabusa series. The relation indicates that volume of active region is B>C>A. Actually, optimized $H_{discharge}$ is different in each thruster, but it is very important to the relation corresponds to the ion beam current, which is one of most important design parameters for the microwave discharge ion thruster.

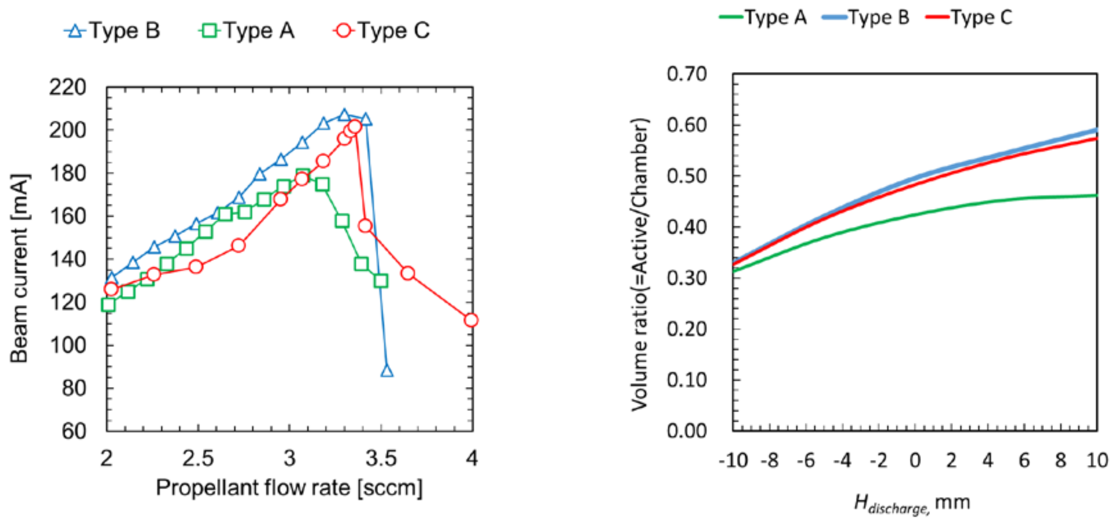

(a) Ion beam current **(b) Normalized volume of active region**

Figure 8. Relationship between ion beam current and volume of active region.

VI.Conclusion

In this study, we investigate the performance limitation of microwave discharge ion thruster µ10 by using full-PIC simulation, DSMC simulation, and electrostatic probe measurement. From the results, the performance limitation is derived that plasma is generated in non-active region. Based on the mechanism of the performance limitation, we suggest that the volume of active region is critical parameter to improve the limitation. Then, we experimented three kinds of thrusters to investigate the relationship between the ion beam current and volume of active region. As a result, the maximum ion beam current corresponds to the volume of active region.

References

1) H. Kuninaka and S. Satori, J. Propul. Power **14**, 1022 (1998).

2) H. Kuninaka, K. Nishiyama, Y. Shimizu, and K. Toki, in Proceedings of 40th AIAA/ASME/SAE/ASEE Joint Propulsion Conference and Exhibit, July 2004, pp. 1–10.

3) K. Nishiyama, T. Hiroyuki, K. Yasuhiro, and A. Tomoko, "DESTINY+ : technology demonstration and exploration of asteroid 3200 Phaethon," 68th Int. Astronaut. Congress (2017).

4) T. Okada, Y. Kebukawa, J. Aoki, J. Matsumoto, H. Yano, T. Iwata, and R.Jaumann, Planet. Space Sci. **161**, 99–106 (2017).

5) John R. Brophy and Paul J. Wilbur, AIAA JOURNAL, **23**, 11, (1985),

6) C. K. Birdsall and A. B. Langdon, Plasma Physics via Computer Simulation (IOP Publishing, Bristol, UK, 1991).

7) K. Nakamura, H. Koizumi, M. Nakano, and Y. Takao, Phys. Plasmas **26**, 043508 (2019).

8) J. P. Verboncoeur, Plasma Phys. Controlled Fusion **47**, A231 (2005).

9) V. Vahedi and M. Surendra, Comput. Phys. Commun. **87**, 179 (1995).

10) Y. Takao, H. Koizumi, K. Komurasaki, K. Eriguchi, and K. Ono, Plasma Sources Sci. Technol. **23**, 064004 (2014).

11) Y. Yamashita, Y. Tani, R. Tsukizaki, D. Koda, and K. Nishiyama, Phys. Plasmas. **26**, 073510 (2019).

12) I. Funaki, H. Kuninaka,K. Toki, and S. Satori, in Proceedings of 34th AIAA/ASME/SAE/ASEE Joint Propulsion Conference & Exhibit (AIAA, 1998), pp. 98–3341.

13) Y. Tani, R. Tsukizaki, D. Koda, K. Nishiyama, and H. Kuninaka, Acta Astronaut. **157**, 425–434 (2019).